International Journal of Infrared and Millimeter Waves, Vol. 27, No. 4, April 2006 (© 2006)
DOI: 10.1007/s10762-006-9103-x

TERAHERTZ HETERODYNE IMAGING PART I: INTRODUCTION AND TECHNIQUES

Peter H. Siegel[1,2] and Robert J. Dengler[2]

[1]*Beckman Institute*
Division of Biology
California Institute of Technology
1200 E. California Blvd
Pasadena, CA 91125
[2]*Submillimeter Wave Advanced Technology*
Jet Propulsion Laboratory
4800 Oak Grove Drive
Pasadena, CA 91109
phs@caltech.edu
Received 00 Month 0000

Abstract

The authors present their ongoing work on terahertz *heterodyne* imaging techniques derived from space science applications and components. In Part I, introductory information and general techniques are provided. Part II contains descriptions of four different heterodyne imaging instruments that have been established at the authors' facilities. In Part III selected applications are discussed. Parts II and III will appear in subsequent issues of this journal.

I. Introduction

The submillimeter-wave regime (300-3000 GHz, 1 mm-100 microns wavelength) and overlapping THz bands (1000-10,000 GHz, 300 to 30 microns wavelength) contain a wealth of largely untapped spectroscopic information from cool, lightweight gases and molecules that have long motivated astronomers and atmospheric chemists to develop remote sensing technology for Earth, planetary and space science applications [1]. Both very narrow bandwidth (<10 MHz) emission and absorption signatures representing rotational, vibrational and librational mode transitions, as well as broad continuum (thermal blackbody) energy provide information on the abundance, distribution, cosmic and local motion of these gases as well as the temperature and pressure of the surrounding environment. For the past four decades submillimeter-wave heterodyne spectroscopy techniques have been used to observe and monitor a wide range of chemical species in planetary atmospheres, including the Earth, as well as comets and moons; detect the presence, size and distribution of water and ice particles (and other large scatterers) in clouds; study regions of new star formation; and analyze the composition, and map the distribution, of gas and dust within our own galaxy and the constituents in the cores of distant galaxies. A noteworthy recent achievement is the detection and identification in the IR of hot (350K) acetylene, hydrogen cyanide and CO_2 around a not-too-distant solar mass proto-star [2]. When combined with water, also found in the interstellar medium, these chemicals catalyze the building blocks of proteins, notably the amino acid adenine [3].

Over the past five years there has been an explosion of interest in the terahertz frequency regime [4]. Applications are widespread and include the biological and biomedical areas [5], security and weapons detection [6], studying fast chemical reactions [7], pharmaceutical screening and drug identification [8], spectroscopy of liquids, solids [9] and hot gases [10], as a tool for studying scattering at much shorter wavelengths [11] and most recently in the communications [12] and radar areas [13]. However the very properties that make this frequency regime so interesting: high absorption from many gaseous species, liquids and solids, especially water, make it extremely difficult for significant penetration or propagation of terahertz energy in almost all Earthly environments, thus severely limiting many of these applications [5, Fig. 1]. Nevertheless, significant progress has been made in the examination of biological and other material samples through the use of ultra-fast-pulse time domain spectroscopy (TDS) [4] and traditional, as well as specialized [14] Fourier Transform Spectroscopy (FTS) techniques. These methods yield wide spectral coverage and reasonable signal-to-noise but, at least in the case of TDS, have limited frequency resolution. As a contrast to TDS and FTS, CW heterodyne radiometry is an old technique that offers the potential for extremely wide dynamic range and high signal-to-noise ratio while maintaining fast data acquisition, stable magnitude and phase measurements, room temperature operation, high amplitude and phase flexibility, simple optical beam forming, active or passive observation modes, use of coherent or incoherent scene illumination, and even the possibility of 3D reconstruction and range finding if electronically swept sources of modest bandwidth can be employed. Heterodyne techniques are at the heart of radio, telecommunications, much of the radar community and a large part of the radio astronomy world. It is not surprising that these same radiometric principles can be used for high quality imaging.

This paper, in three parts, reviews some of the motivations, techniques, and applications for imaging using CW heterodyne methods. Part I is a general introduction to heterodyne imaging and discusses sensitivity issues and some desirable and undesirable characteristics of the technique. Part II presents detailed information on four different heterodyne imaging systems that have been set up in the author's laboratories. In the third article, specific applications for these heterodyne imaging instruments, both in space science and for general applications in biology and security are discussed. We pay particular attention to those application areas where heterodyne imaging might offer some unique advantages over other methods, or where significant synergy exists to warrant the deployment of complementary systems such as Fourier transform and fast-pulsed time domain spectrometers. This set of articles is meant only as a narrowly focused introduction to this rapidly evolving field and the interested reader should keep a close watch on the relevant conference and journal publications (not always typical of the TDS and FTS imaging communities) that currently include terahertz *heterodyne* instruments and techniques, some of which are listed in [15].

II. Heterodyne Technique

Heterodyning (literally *other or different power*), the beating together of two closely spaced frequencies to yield the sum and difference of the original signals, has been around for over 80 years - since the very early days of radio [16]. The chief advantage is in the acquisition of very weak, narrow-band signals where direct detection and post amplification, or pre-amplification followed by detection, adds so much electronic noise that the signal cannot be recovered without prohibitively long integration times. Since the integration time required to reach a minimum detectable signal or temperature difference increases as the square of the equivalent system noise temperature (see section III), it is important to minimize all sources of spurious electronic fluctuation. At frequencies above approximately 150 GHz, electronic pre-amplification of weak signals is not yet possible[1] [17] and the heterodyne process, wherein the signal is first converted to a much lower frequency using the difference beat note (intermediate frequency or IF) supplied by a local source of radio frequency (RF) energy (local oscillator or LO) at a closely spaced frequency (generally in the microwave band, i.e. 1-30 GHz), is preferred. The conversion process is accomplished through a *mixer* [18], generally composed of some form of nonlinear rectifying element (diode, fast bolometer, tunnel junction etc.) that is operated like a current or voltage (or thermal) switch whose Fourier components include, and are optimized (via circuit implementation), to enhance the difference frequency signal (IF). Once the signal has been converted to the IF, electronic amplification is available to boost the output power without adding too much additional noise. The signal can now be easily filtered, distributed, down converted a second or third time if need be, and finally detected. The bandwidth and stability of the down converted signal depends on that of the LO, which is often frequency or phase locked to a microwave reference through a harmonic mixer, or generated directly from a high stability synthesizer (using frequency up converters or multipliers). If the reference oscillator is very narrow band, and the output frequency is filtered, thermal noise or unwanted signals surrounding the desired RF, that are generally incident upon the detection element, can be dramatically reduced (especially useful when the signal itself is band limited – such as all low pressure gas emission lines)[2]. This ability to match the detection bandwidth to the inherent signal bandwidth is what makes the heterodyne process so appealing. Signal bandwidth filtering can be taken to

[1] Low noise pre-amplifiers in this frequency range are just beginning to be developed, and above 100 GHz they are not yet competitive with direct heterodyning. This is likely to change in the near future and, at least up to 300 GHz, pre-amplification and detection or pre-amplification followed by down conversion soon may be available.

[2] Note however that in the mixing process, RF signals on both sides of the LO (LO+IF or upper sideband and LO-IF or lower sideband) generally will be equally well down converted to the IF unless the mixer is tuned to reject one or the other (image reject mixer). This sideband folding can be used to advantage if desired signals exist on both sides of the LO or it can limit the ultimate receiver sensitivity as noise in the unwanted sideband will appear in the IF.

great extremes (it is not uncommon to have a total RF bandwidth of only a few hundred kHz, i.e. 1 part in 10^7) and thus extremely high signal-to-noise systems are possible – 100 dB or more. This is the major reason many astronomical instruments that are designed to measure thermal emission or absorption from low pressure gases are implemented as heterodyne receivers. For continuum or broader bandwidth spectroscopy or imaging, direct detection systems (generally cooled to reduce inherent thermal noise and optically filtered to reduce the background noise bandwidth) are preferred. Heterodyne systems based on room temperature detectors, such as Schottky barrier diodes, have one other inherent advantage – extremely wide dynamic range. Signals as small as a picowatt or as large as several milliwatts can generally be measured, and remain linear (square law relationship between incident power and detected current or voltage), within the same receiver. For most imaging applications it is not necessary to have a dynamic range of 10^{10}, however since absorption is such a large problem in the terahertz bands, having a very large available range makes calibration as well as imaging over objects with very high differential contrast (wide range of emissivity), or even glint, much easier. Other demonstrated advantages of the terahertz heterodyne process include preservation of magnitude and phase information; the ability to filter to arbitrarily narrow output bandwidths or utilize a broad IF (>20 GHz); electronic tuning over significant (~20%) RF bandwidths; immunity from signals outside the designated input band; linearity over wide dynamic range; and electronic beam steering or beam combining by manipulation of signals at the microwave IF rather than at the terahertz RF.

III. Heterodyne Sensitivity

The choice of employing one or another sensing system and detector type is generally application based. An excellent review of submillimeter wave receiver systems, detectors, figures of merit and performance limitations, still relevant after almost 30 years, can be found in [19]. When available signal power levels are low (near or below the thermal background noise) two types of CW integrating receivers are generally employed in the terahertz range: direct detection, or video receivers, and rectifying, or heterodyne systems. Illustrative block diagrams are shown in Fig. 1. Direct detection receivers, both inherently (based on their field of view and frequency responsivity), and artificially (through the use of predetection filters and input mode matching antennas), limit the total thermal energy from the scene that falls on the detector element. A heterodyne receiver limits this thermal energy through an intermediate frequency or *post-conversion,* rather than pre-detection, filter. In order to compare the background sensitivity limitations in the two types of receivers, we can use the example of a constant temperature object that completely fills the field of view of the instrument, which for the sake of discussion is set up to detect all modes (for a classic article on sensitivity in infrared thermal and photoconductive detectors see Putley [20] or a very nice recent discussion by De Lucia [21]). A helium cooled detector of area A m^2 looking straight up at this constant temperature environment T, with a cooled filter on the input of bandwidth $B_{in}=f_2-f_1$ and $f_c=f_1+B_{in}/2$ accepting a cone

of radiation Ω from the scene, sees a background limited power level (excludes any internal detector or external amplifier noise) given by [20 eqn. (5)]:

$$P_{NBackground} = \frac{2(kT)^{5/2}}{ch^{3/2}}\left(A\Omega B_{out}[J_n(x_2) - J_n(x_1)]\right)^{1/2},$$

$$J_n(x_m) = \int_0^{x_m} \frac{x_m{}^n e^{x_m}}{(e^{x_m}-1)^2} dx \quad \text{and} \quad x_m = hf_m/(kT), \text{ where } n=4 \text{ and } m=1,2.$$

Here B_{out} is the integration bandwidth (typically 1 Hz), k is Boltzmann's constant, h is Planck's constant and c is the speed of light (mks units). The integrals can be evaluated with MathCAD® for instance. The equation is valid for thermal detectors only and must be modified slightly for photoconductive detectors (typically lowers $P_{NBackground}$ by ~2 [20 eqn. (7)]), or dramatically if the detector is in an ambient environment where its own thermal noise (unfiltered by B_{in}) is present [20 eqn.(2)]. For purposes of comparison, $P_{Nbackground}$ for several typical detector cases is tabulated in Table I. The point is to compare the results under different input and output bandwidth conditions and operating environments. From the table it is easy to see where heterodyne detectors come into play. In an environment where the noise power from the scene is the limiting sensitivity parameter, the narrow band input frequency range inherent with heterodyne techniques makes these detectors less likely to be background noise limited. It should be noted, as is clearly pointed out in [21], that the *total radiant* power in the scene for the cases shown in Table I is larger than the background noise power, and that these detectors have no problem measuring a strong signal in such ambient environments.

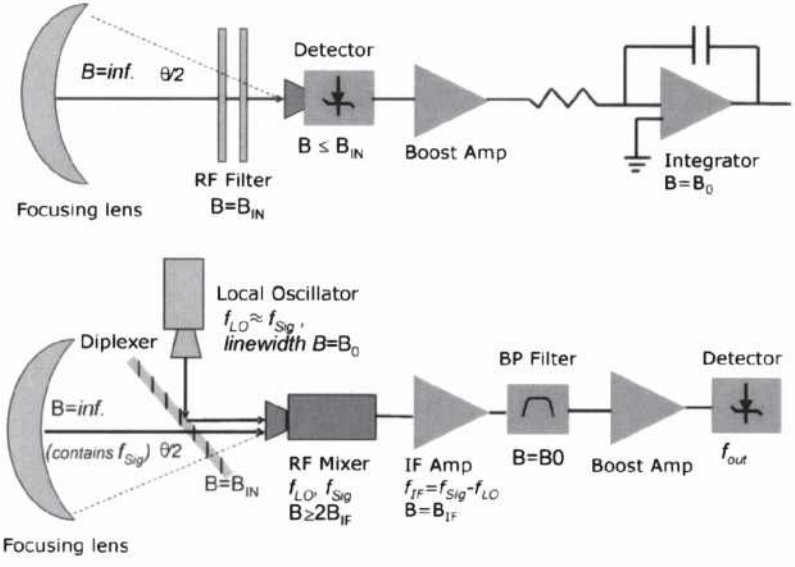

Fig. 1. Simplified schematic diagrams of (top) typical direct detection system and (bottom) typical heterodyne system for submillimeter wave applications.

Table I. Background Limiting Noise for Detectors

DETECTOR DESCRIPTION AND CONDITIONS	$P_{N\,Background}$ (W)
Helium Cooled Bolometer with f_{center}= 1THz, **B_{in}=100 GHz**, Bout=1 Hz, A=1 cm^2, Ω= 30 degrees, T_{scene}= 300K, multimode	**1.1×10^{-13}**
Helium Cooled Bolometer with f_{center}= 1THz, **B_{in}=1000 GHz**, Bout=1 Hz, A=1 cm^2, Ω= 30 degrees, T_{scene}= 300K, multimode	**3.6×10^{-13}**
Helium Cooled Bolometer with f_{center}=1 THz, **Bin= 1 GHz**, Bout=1 Hz, A=1 cm^2, Ω=30 degrees, T_{scene}=300K, multimode	**1.1×10^{-14}**
Helium Cooled Bolometer with f_{center}=1THz, Bin=100 GHz, Bout=1 Hz, A=1 cm^2, Ω=30 degrees, **T_{scene}[1]=10K,** multimode	**3.2×10^{-16}**
300K Bolometer[2] with f_{center}=1 THz, Bin= 100 GHz, Bout=1Hz, A=1 cm^2, Ω=30 degrees, T_{scene}=300K, multimode	**3.9×10^{-11}**
Helium Cooled Bolometer with f_{center}=1 THz, **Bin= 1 GHz**, Bout=1 Hz, A=1 cm^2, Ω=30 degrees, T_{scene}=300K, **single mode[3]**	**2.3×10^{-16}**

[1] Cool background, as in star forming regions in outer space
[2] Dominated by unfiltered detector self thermal energy
[3] Input power limited to a single mode as in a heterodyne detector so that: $A\Omega \approx \lambda^2$ [19].

$P_{Nbackground}$ is only part of the story. The most common figures of merit for a detector system used for imaging in a thermal environment are the minimum detectable signal or Noise Equivalent Power (NEP) and the minimum detectable temperature difference that can be measured in the scene (noise equivalent delta temperature or NEΔT). NEP is generally dominated by the electrical noise in the detector system and includes current or voltage fluctuations in the detector element, external amplifier noise contributions, and in practice, may include input or output mismatch from the detector to the mode matching antenna or from optical elements in the system. NEΔT takes into account the total integration time and output bandwidth as well as optical losses.

The NEP is the smallest detectable change in input signal power that produces a change in output power equal to the RMS fluctuations in the output signal in an arbitrarily fixed bandwidth of 1 Hertz, i.e. a signal-to-noise ratio (S/N) of unity. Since these fluctuations in output signal are generally proportional to the square root of the output bandwidth, B_{out} (typical of thermal noise for example), NEP is expressed in Watts per root Hertz or W/Hz$^{1/2}$. For most video detectors the NEP

is a measured quantity and is dependent on the post-detection amplifier and $1/f$ noise, the noise in the detector itself (usually thermal or Johnson noise associated with the detector resistance), and the detector responsivity. For comprehensive reviews see Wood [22] or Richards [23]. The responsivity is typically a measure of the output voltage produced by a given input signal and has units of V/W. In the mid and near IR, thermal detectors typically take the form of small area sheet absorbers that respond to all modes incident on them from the scene (# modes $\approx A\Omega/\lambda^2$, A=area of detector, Ω=solid angle, λ=wavelength). In the far IR however the bolometer area necessarily becomes quite large for most modest f-number systems and RF antennas are imposed between the detector element and the scene in order to achieve diffraction limited performance [24]. This helps from the point of view of background limited sensitivity, since the antenna serves as a mode filter (# modes=1 or 2 for dual polarization), and also enhances both responsivity and response time [25]. For these systems the optical NEP (which includes all mode converting antennas and filters as well as optical losses in the beam forming network and background noise) seems to be a better measure for comparing systems, than the often quoted detector NEP.

Many types of thin film, and composite (antenna coupled microbolometers) have been developed for both room temperature [22] and cooled operation but only a few uncooled systems have been employed at THz frequencies [24,25,26,27]. The remainder have tended to be superconducting transition edge [28], hot electron [29], tunnel junction [30], or recent silicon nitride micromesh bolometers [31,32] which have the sensitivity required for astronomical detector applications (cold background)[3]. Ultra high sensitivity photon counting devices (single electron transistors based on quantum dots) have also been constructed and tested at Terahertz frequencies with even lower NEPs [33,34].

The best room temperature results in the subterahertz bands that have been reported use antenna coupled niobium microbridge bolometers [27,35,36] which have optical NEPs measured at 100 GHz of approximately 10^{-11} W/Hz$^{1/2}$. Vanadium oxide and other thin films have somewhat better reported mid IR performance [37] but the authors are unaware of any terahertz results for these detectors. Some earlier bismuth results [24,25] are also quite reasonable. For comparison a commercial Golay cell [38] (based on detecting the movement of a diaphragm caused by a change in volume of a gas filled cavity as it is heated by incoming radiation) has an optical NEP of approximately 10^{-10} in this wavelength range. Past commercial GaAs Schottky barrier diode detectors had NEPs of about 3×10^{-9} at 1 THz. [39]. Cooled bolometers looking at 300K are generally background limited and require cooled optics as well as a cold background to perform at

[3] In outer space, where the background is around 10K, the full advantage of the high sensitivity detectors can be realized so long as the optical elements of the receiver are also cooled (to eliminate in-beam radiant energy) and any stray warm radiant energy from sources outside the main beam are prevented from entering the receiver .

maximum possible sensitivity. The limiting NEP in a heterodyne system is determined by the total system noise temperature which contains the noise temperature of the down converting or rectifying element (typically dominated by thermal and shot noise, or in the case of very sensitive superconducting detectors, by quantum noise), the efficiency in shifting power from the input RF to the IF, the noise and gain of the first stage post-conversion IF amplifier, and losses in the optical elements plus background spillover. At frequencies at or below 150 GHz, low noise pre-conversion or pre-detection amplifiers are now becoming available for both heterodyne and direct detection systems [40,41]. In this case the NEP is usually dominated by the noise in this first stage amplifier. Typical NEPs for a variety of room temperature and cooled systems are given in Table II.

Table II. Optical NEP for Some Direct Detectors and Heterodyne Systems

SYSTEM DESCRIPTION	NEP ($W/Hz^{1/2}$)	Comments
Nb microbridge **room temperature** composite bolometer, T_{bath}=**300K**, f_{in}=0.1 THz, Ref.[35]	$1x10^{-11}$	Results at 100 GHz
Bismuth **room temperature** composite bolometer, T_{bath}=**300K**, f_{in}=2.5THz, Ref. [24]	$1.6x10^{-10}$	Degrades in air
Vanadium oxide **room temperature** thin film bolometer T_{bath}=**300K**, f_{in}=30 THz, Ref. [37]	$<1x10^{-11}$	No data below 30 THz
Golay Cell, **room temperature** T_{bath}=**300K**, f_{in}=0.1-1 typical THz, Ref. [38]	$1x10^{-10}$	Commercial spec.
Schottky Diode Detector, **room temperature** T_{bath}=**300K**, f_{in}=0.6-1 THz, Ref. [39]	$3x10^{-9}$	Perf. poorer above 1 THz
Nb micro-bridge **superconducting** bolometer T_{bath}=**4K**, f_{in}=0.1-1 THz, Ref. [36]	$4x10^{-13}$	Device NEP 10X lower
Transition edge **superconducting** bolometer T_{bath}=**0.3K**, f_{in}=0.2-0.3 THz, Ref. [23]	$<10^{-16}$	Most popular bolometers
Hot electron **superconducting** micromesh bolometer T_{bath}=**0.1K**, f_{in}=1 THz, Ref. [31]	$3x10^{-17}$	Space qualified
Single electron transistor T_{bath}=**0.05K**, f_{in}=1-3 THz, [34]	$<1x10^{-17}$	Also requires high B fields
Schottky Diode **Mixer**[1]: **Room Temperature** T_{bath}=**300K**, f_{in}=0.5 THz	$3.9x10^{-15}$	Best commercial
Schottky Diode **Mixer**[2]**: Room Temperature** T_{bath}=**300K**, f_{in}=**2.5 THz**	$1.5x10^{-14}$	Space qualified

[1] Mixer assumptions: T_{mixer}=1500K at 300K ambient, $T_{IF\ amp}$=25K, Conversion Loss=8dB, 300K background, B_{IF} =4 GHz, 1.1dB optical losses, giving T_{sys} (DSB)=2220K, and for a 1 second integration time τ and 1 Hz output bandwidth: $NEP=2kT_{sys}B_{IF}^{1/2}/(B_{out}\tau)^{1/2}$ (see text).

[2] Mixer Assumptions: T_{mixer}=5000K; $T_{IF\ amp}$=25K, Conversion Loss=10 dB, optics losses=1.1 dB, B_{IF} =6 GHz, yielding T_{sys} (DSB)=6850K. Based on performance data of flight qualified JPL mixer operating at 2520 GHz.

Note that the room temperature heterodyne mixers have NEP values that exceed those of the helium (4K) cooled direct detectors for narrow input band detection (4 and 6 GHz shown).

A good figure of merit for the sensitivity of imaging systems is the smallest noise equivalent temperature change that can be measured in a scene in a given integration time. This expression, Noise Equivalent Delta Temperature, NEdT or NEΔT, is related to the NEP by [19 with output bandwidth included]:

$NE\Delta T_{Het} = NEP \cdot B_{out}^{1/2} / (2kB_{IF}) = T_{sys} / (B_{IF}\tau)^{1/2}$ in a heterodyne system[4] and

$NE\Delta T_{Dir} = NEP \cdot B_{out}^{1/2} (\lambda^2/2E)/(kB_{in}) \approx T_{sys}/ (B_{IN}\tau)^{1/2}$ for direct detection[5].

NEΔT is measured in K and is an important figure of merit for imaging because it associates a minimum detectable contrast difference with an allotted integration time τ and output bandwidth B_{out}. $\lambda^2/2E$ is a measure of the number of received modes where $E=A\Omega$ is the Etendue or detector area times the effective solid angle of the observed signal. For antenna coupled systems, E is typically λ^2 (single mode, one polarization) or $2\lambda^2$ (two polarizations), and the difference in NEΔT between heterodyne and direct detection systems reduces to the ratio of input, B_{IN}, to intermediate frequency, B_{IF}, bandwidth: $NE\Delta T_{Het}/NE\Delta T_{Dir} \approx B_{IN}/B_{IF}$. Hence when wideband signals are being observed, as in the case with thermal or blackbody power, direct detection systems with $B_{IN} >> B_{IF}$ will have higher sensitivity. The opposite will be the case when the signal has a limited bandwidth and the direct detector responds to frequencies much wider than that of the signal itself.

Examples of the NEP and NEΔT for different detection systems are tabulated in Table III. The first realized systems above 100 GHz with large numbers of pixels (64x128) were the highly integrated silicon based microbolometer arrays developed by Honeywell. The reported NEΔT for deployed room temperature units is below 0.25K out to 14 microns wavelength [22] and even lower (<0.1K) for larger arrays of 160x120 pixels [37]. Nothing equivalent to these large scale arrays yet exists in the submillimeter, although a large scanned array system is being developed for 650 GHz using niobium microbridge bolometers at NIST [42].

---

[4] A simpler way to look at this is to set the signal-to-noise, S/N=1 in both direct and heterodyne systems where:
$S/N_{Het} = T_{sce}/T_{sys} (B_{IF}\tau)^{1/2}$ – the radiometer equation, and:
$S/N_{Det} = 2kT_{sce}B_{IN}\tau^{1/2}/NEP$ - the defining NEP equation for direct detection single mode systems.
Then T_{sce} becomes the minimum detectable temperature or temperature difference in the scene:
$T_{sce}(\min) \equiv NE\Delta T_{Het} = T_{sys}/(B_{IF}\tau)^{1/2}$ for the heterodyne system and,
$T_{sce}(\min) \equiv NE\Delta T_{Dir} = NEP/(2kB_{IN}\tau^{1/2})$ for the direct detection system.

[5] Valid only if $B_{in} << f$, the signal frequency, and we are in the Rayleigh Jeans regime.

Table III. NEP and NEΔT for Direct and Heterodyne Imagers with 1 Pixel

Detector Type	B_{IN} GHz	B_{IF} GHz	T_{sys} DSB K	NEP_0 W/Hz$^{1/2}$	NEΔT K
300K Mixer	1	1	2960	2.8×10^{-15}	0.10
300K Mixer	100	10	3190	9.4×10^{-15}	0.034
300K Mixer	100	100	4100	3.8×10^{-14}	0.014
77K Mixer	1	1	1830	1.8×10^{-15}	0.065
4K HEB Mixer	1	1	670	7.6×10^{-16}	0.023
300K Bolometer	1000	1 Hz	3.6×10^{5}	1×10^{-11}	0.36
300K Bolometer	100	1 Hz	1.1×10^{6}	1×10^{-11}	3.6
300K Bolometer	10	1 Hz	3.6×10^{6}	1×10^{-11}	36.2
300K Bolometer	1	1 Hz	1.1×10^{7}	1×10^{-11}	362
4K Bolometer	1000	1 Hz	1.4×10^{4}	4×10^{-13}	0.015
4K Bolometer	100	1 Hz	4.5×10^{4}	4×10^{-13}	0.15
4K Bolometer	10	1 Hz	1.4×10^{5}	4×10^{-13}	1.5
4K Bolometer	1	1 Hz	4.6×10^{5}	4×10^{-13}	14.5

Assumptions: Single pixel receiving single mode with 1 sec integration time, output bandwidth of 1 Hz and input/IF bandwidths as shown and a sky temperature (background) of 200K. Values of $T_{sys}=T_{mixer}+LT_{IF}$ derived from typical results near 650 GHz with T_{mixer} =1800K DSB, L=8dB, T_{IF} =25/50/150K for B_{IF}=1/10/100 GHz, $T_{77K\ Mixer}$=1000K, L and T_{IF} as before, T_{HEB}=200K, L_{HEB}=8dB, warm optics (290K) and 1.6dB optics losses ahead of the mixer and T_{IF}=25K. Note that for these scene temperatures the cooled HEB mixer is background limited (T_{sys} dominated by sky and optics losses). The NEP for the heterodyne system is calculated from T_{sys} using $NEP=2kT_{sys}B_{IF}^{1/2}/(B_{out}\tau)^{1/2}$. Values of T_{sys} for the detectors are obtained from the NEPs in Table II using $T_{sys}=NEP(B_{out}\tau)^{1/2}/(2kB_{IN}^{1/2})$ and assuming the fixed NEPs shown as B_{IN} varies.

The advantage of heterodyne detection when the limiting factor is no longer the noise power from the scene is apparent from Table III. This is the case when the input bandwidth is set by the inherent nature of the signal, as with emission lines from low pressure gases or direct illumination of the scene by a coherent narrowband source. In this instance room temperature heterodyne systems can have NEΔT well in excess of helium cooled direct detection systems. Cooled heterodyne systems are even more advantageous. In a real application however many other considerations enter in, including the cost and complexity of the components as well as the ease in which the outputs of the detector elements can be combined to form an image, assuming more than a single scanned pixel is desired. Other general advantages of the heterodyne approach are:

(1) Heterodyning preserves the magnitude and phase of the original signal because the detection occurs after the downconversion process and at a frequency where signal amplification or manipulation is straight forward.
(2) Heterodyne systems (at least those employing devices that don't behave bolometrically) typically operate at intermediate frequencies above the $1/f$

knee for electronic devices, avoiding some inherent output detector noise that can be present in slower responding detectors.
(3) Heterodyne systems do not generally require signal chopping since post amplification provides very high signal-to-noise, however frequent signal path gain calibration may be required (using calibrated signal or noise power sources) to maintain linearity and amplitude stability.
(4) A heterodyne system can have very large dynamic range because rectifying down conversion elements generally handle large power levels (tens of milliwatts)[6] and have low intrinsic noise levels (below -90 dBm). Even at 2.5 THz, over 100 dB of dynamic range has been easily obtained with room temperature Schottky diode downconverters or mixers [43].
(5) In a heterodyne system the IF bandwidth can be readily designed either to match a narrow band signal, minimizing output noise, or be expanded to increase signal power (for wider band or blackbody sources) or to detect multiple closely spaced signals, by distributing the broad IF to a set of narrowband filters and individual detectors - a filter bank or spectrometer.
(6) A heterodyne system can generally be designed to perform a fast narrow band frequency sweep over a scene – either using a single filter scanned across a broad IF (LO fixed, RF-LO varying across the IF band) or using a fixed IF and a scanned local oscillator (LO-RF fixed, LO and signal varying across the RF band) - thereby recording the phase and amplitude change in a signal that is emanating from a spatially fixed object or the Doppler shift resulting from a moving object. The ability to use very narrow detection bandwidth (1 part in 10^7 typical) gives high phase or velocity accuracy.

Although direct detection CW systems are generally more sensitive for applications involving the measurement of broad thermal energy, and they are much more easily configured in arrays because they do not suffer the complication of having to diplex two very high frequency signals (LO plus RF) or provide low loss output coupling of a relatively high frequency microwave signal (IF); they generally require cooling to match the performance of heterodyne systems operating at room temperature at THz frequencies, and they lack some of the signal processing flexibility inherent in working with the phase coherent microwave signals present in heterodyne systems. Heterodyne instruments are well understood, relatively straight forward to construct, have sophisticated signal processing capabilities, and are common elements in almost all microwave communications circuits (meaning that at least for IF processing, components are cheap and abundant). In Part II of this paper we take a look at some examples of several heterodyne imaging systems the authors have set up for operation in the THz regime, their configuration and their performance.

[6] Note that this is not necessarily for superconducting or bolometric devices, which generally have much lower NEP but also saturate at lower input power levels.

IV. Summary and Comments

In Part I of this paper we have introduced the methodology and some of the performance drivers for heterodyne imaging at Terahertz frequencies. As can be seen from companion articles in this issue, there are many other methods that can be employed to perform imaging at these wavelengths. As with all applications, the particular approach and realization depend upon imposed constraints, whether they be functional, environmental, technical or financial. In space applications even large differences in performance are often outweighed by technical risk, component reliability, mass and power. In rare cases, only a single technique can provide the required data. This is certainly not true in the case of terahertz imaging. Advantages of the heterodyne technique are most pronounced when imaging is performed with very narrow band sources, whether they be naturally occurring interstellar molecular line emissions or artificially generated coherent scene illuminators. In these cases extremely wide dynamic range, high frequency resolution and at least below 1 THz, all solid-state construction are hallmarks of this technique. Although, as will be apparent in Part II, some of the electronic circuits employed in the microwave and backend spectrometer portions of the instruments may seem component rich or complex in comparison with FTS or TDS methods, in fact the enormous wealth of signal processing, RF integrated circuit and commercial microwave resources that have grown up over the last 50 years make this portion of the instrumentation relatively simple, compact and low cost. This is not yet the case for the submillimeter wave components (sources and receivers), which although only a few are required, remain relatively rare, and therefore extremely costly. The most ideal operating frequency for many of the applications that have been proposed for ground based or low flying aircraft terahertz imaging systems seems to be either the 650 or 850 GHz atmospheric windows. These wavelengths offer a good compromise between system performance, scene resolution and aperture size. Higher frequency systems may offer particular contrast advantages, (more likely for active rather than passive imaging) depending on materials being examined and desired penetration depths. Swept or chirped frequency heterodyne systems offer many of the same features as TDS systems (all microwave network analyzers offer time domain measurements as a secondary capability) and therefore should not be discounted when considering 3D scene reconstruction or any of the techniques common in the radar community. The most important advance, in the author's opinion, for heterodyne imaging will come when a fully implemented 2D staring array is demonstrated. Meanwhile, simple single or few pixel systems will have to suffice.

Acknowledgements

The authors would like to thank the many past and present members of the Submillimeter Wave Advanced Technology (SWAT) team at JPL, who participated in developing, setting up and working with the various heterodyne imaging sys-

tems or components that are described in this series of papers. Of particular mention are: Dr. Imran Mehdi, Dr. Anders Skalare, Dr. Frank Maiwald, Dr. Lorene Samoska, Mr. John Oswald, Dr. Hamid Javadi, Dr. Erich Schlecht, Dr. Goutam Chattopadhyay, Dr. John Ward, Dr. John Gill, Dr. Michael Gaidis, Mr. Robert Lin, Mr. David Pukala, Mr. Jim Velebir, Mr. Ray Tsang, and Mr. Ed Luong. Other significant contributors at JPL include: Dr. John Pearson, Dr. Herb Pickett, Dr. Paul Stek and Mr. Peter Bruneau (fabrication). Acknowledgement is also extended to Caltech undergraduate student Tom Tsai for help with our imaging experiments during the summer of 2005. Very special thanks go to Prof. X-C. Zhang of RPI for stimulating our work on the MVNA system that will be described in Part II, during his recent stay at JPL as a Distinguished Visiting Scientist. Finally, we thank Erich Grossman, NIST Boulder, for the preprint and references on his niobium microbridge bolometer work. This work was carried out at the California Institute of Technology Jet Propulsion Laboratory under contract from the National Aeronautics and Space Administration with additional funding from the National Institute of Health under grant K25 EB00109-01 to the California Institute of Technology Division of Biology.

References

[1]. P.H. Siegel, "THz Technology," IEEE Trans. Microwave Theory and Techniques 50th Anniversary Issue, vol. 50, no. 3, pp. 910-928, March 2002.

[2]. F. Lahuis, E.F. van Dishoeck, A.C.A. Boogert, K.M. Pontoppidan, G.A. Blake, C.P. Dullemond, N.J. Evans, M.R. Hogerheijde, J.K. Jørgensen, J.E. Kessler-Silacci and C. Knez, "Hot Organic Molecules Toward a Young Low-Mass Star: A Look at Inner Disk Chemistry," The Astrophysical Journal Letters, v. 636, L145–L148, Jan. 10, 2006.

[3]. Prof. Geoff Blake, Caltech Cosmochemist, private communication.

[4]. See for example any of four recent texts: Sensing with Terahertz Radiation, Dan Mittleman, Editor, Springer Verlag Series in Optical Sciences v. 85, Berlin, 2003. Terahertz Sensing Technology, Vol. 1 and Vol. 2, D. L. Woolard, W.R. Loerop and M.S. Shur, Editors, World Scientific Selected Topics in Electronics and Systems vols. 30 and 32, Singapore, 2003 and 2004. Terahertz Optoelectronics, K. Sakai, Editor, Springer Topics in Applied Physics, Berlin, 2005.

[5]. P.H. Siegel, "THz Technology in Biology and Medicine," IEEE Trans. Microwave Theory and Techniques, vol. 52, no. 10, pp. 2438-2448, Oct. 2004.

[6]. See for example the many papers in the last four SPIE Defense and Security Symposia annual conference series on Terahertz for Military and Security Applications.

[7]. C. Schmuttenmaer, "Exploring dynamics in the far-infrared with tera-

hertz spectroscopy," Chem. Rev. v. 104, pp.1759-1779, April 2004.

[8]. See for example many nice papers by the group at Teraview Ltd. such as: V. P. Wallace, P.F. Taday, A.J. Fitzgerald, R.M. Woodward, J. Cluff, R.J. Pye, and D.D. Arnone, "Terahertz pulsed imaging and spectroscopy for biomedical and pharmaceutical applications," Royal Chem. Soc., Faraday Discussions no. 126, pp. 255-63, 2004, and papers from groups led by K. Kawase, Nagoya University, Japan, for example: K. Kawase, Y. Ogawa, Y. Watanabe, "Terahertz spectroscopic imaging and its application to drug detection," IEICE Trans. on Electronics, vol. E87-C, no. 7, pp. 1186-91, July 2004.

[9]. See the many papers in the last two years of the Int. Conf. on Infrared and Millimeter Waves (IRMMW), and for example: T. Globus, et.al., "Terahertz Fourier transform characterization of biological materials in solid and liquid phases," SPIE Symposium on Chemical and Biological Standoff Detection, SPIE vol. 5268, no. 1, pp. 10-18, 2003.

[10]. R.A. Cheville, R.A., D. Grischkowsky, "Far-infrared terahertz time-domain spectroscopy of flames," Optics Letters, vol. 20, no. 15, pp. 1646-8, 1 Aug. 1995.

[11]. J. Pearce, D.M. Mittleman, "Using terahertz pulses to study light scattering," Physica B, vol. 338, no. 1-4, pp. 92-6, Oct. 2003.

[12]. See for example papers from NTT Japan such as: T. Nagatsuma, et.al., "Sub-terahertz wireless communications technologies," Teratech Proceedings, Osaka, Japan, Nov. 2005, *or* M.J. Fitch and R. Osiander, "Terahertz waves for communications and sensing," Johns Hopkins APL Technical Digest, vol. 25, no.4, pp. 348-55, Oct.-Dec. 2005.

[13]. See for a start: E.R. Brown, "Fundamentals of Terrestrial Millimeter-Wave and THz Remote Sensing," in Terahertz Sensing Technology, Vol. 2, D. L. Woolard, W.R. Loerop and M.S. Shur, Editors, World Scientific Selected Topics in Electronics and Systems, vol. 32, Singapore, 2004.

[14]. D.T. Petkie, T.M. Goyette, R.P.A. Bettens, S.P. Belov, S. Albert, P. Helminger and F.C. De Lucia, "A fast scan submillimeter spectroscopic technique," Review of Scientific Instr., vol. 68, no. 4, pp. 1675-1683, April 1997.

[15]. Journal of Infrared and Millimeter Waves, Elsevier Publishing and associated annual conference; Int. Symposium on Space THz Technology (http://www.space-thz.org); IEEE Microwave Theory and Techniques and associated annual Int. Microwave Symposium; European Microwave Conference; SPIE Proceedings on Astronomical Telescopes and Instrumentation; SPIE Defense and Security Symposium – Assorted Special Sessions on Terahertz Sensors and Imaging.

[16]. Tom Lewis, "Empire of the Air, The Men Who Made Radio," Harper Collins, NY, 1991.

[17]. See papers in the 2006 IEEE MTT-S Int. Microwave Symposium, Focused Session on Terahertz Integrated Circuits, San Francisco, CA, June 11-16, 2006.

[18]. See for example the classic Radiation Lab series texts: Crystal Rectifiers, by Torrey and Whitmer; Microwave Mixers, by Pound; Microwave Receivers, by Van Voohris; and Threshold Signals, by Lawson and Uhlenbeck; all from the MIT Radiation Laboratory series, L. Ridenour and G. Collins, editors, McGraw Hill, 1950, *or* a more recent textbook by Steven A. Maas: Microwave Mixers, Aertech House, Boston, 1993.

[19]. T. G. Blaney, "Radiation detection at submillimeter wavelengths," Journal of Physics E (Scientific Instruments), v. 11, pp. 856-881, Sept. 1978.

[20]. E. H. Putley, "The ultimate sensitivity of sub-mm detectors," Infrared Physics, v. 4, issue 1, pp. 1-8, March 1964.

[21]. F. C. De Lucia, "Noise, detectors, and submillimeter-terahertz system performance in nonambient environments," J. Opt. Society of America B, v. 21, no. 7, pp. 1273-1279, July 2004.

[22]. Andrew Wood, "Monolithic Silicon Microbolometer Arrays," Uncooled Infrared Imaging Arrays and Systems, v.47 of Semiconductors and Semimetals, Academic Press, pp. 43-122, 1997.

[23]. P.L. Richards, "Bolometers for infrared and millimeter waves," J. Appl. Phys., vol. 76, no. 1, pp. 1-24, July, 1994.

[24]. T. Hwang, S.E. Schwarz and D.B. Rutledge, "Micorbolometers for Infrared Detection," Appl. Phys. Lett., v. 34, no. 11, pp. 773-776, June 1, 1979.

[25]. S.M. Wentworth and D. Niekirk, "Far-Infrared Composite Microbolometers," IEEE MTT-S Digest, Dallas, TX, paper pp-3, pp. 1309-1310, June 1990.

[26]. C. Ling, J. Laundry, H. Davee, G. Chin and G.M. Rebeiz, "Large area bolometers for THz power measurements," IEEE. Trans. Microwave Theory and Tech., v. 42, no. 4, pp.758-760, April 1994.

[27]. A. J. Miller, A. Luukanen, A. and E.N. Grossman, "Micromachined antenna-coupled uncooled microbolometers for terahertz imaging array," Proc. SPIE v. 5411 pp.18-24, 2004.

[28]. J. Clarke, P.L. Richards, P.L, N.H. Yeh, "Composite superconducting transition edge bolometer," Applied Physics Letters, vol. 30, no. 12, pp. 664-6, 16 June 1977.

[29]. B.S. Karasik, W.R. McGrath, H.G. LeDuc and M.E. Gershenson, "A hot electron direct detector for radioastronomy," Superconducting Science and Tech., vol. 12, pp. 745-747, Dec. 1999.

[30]. H. Matsuo, S. Ariyoshi, M. Takeda and T. Noguchi, "SIS photon detectors for submillimeter-wave observations," Twelfth Int. Sym. on Space THz Tech., San Diego, CA, page 476, Feb. 14-16, 2001.

[31]. A. Turner, J. Bock, J. Beeman, J. Glenn, P. Hargrave, V. Hristov, H. T. Nguyen, F. Rahman, S. Sethuraman and A. Woodcraft, "Silicon nitride micromesh bolometer array for submillimeter astrophysics," Applied Optics, v. 40, no. 28, pp. 4921-32, Oct. 2001.

[32]. P. D. Mauskopf, J. J. Bock, H. Del Castillo, W. L. Holzapfel, A. E. Lange, "Composite infrared bolometers with Si3N4 micromesh absorbers," Applied Optics, vol. 36, no. 4, pp. 765-771, Feb. 1997.

[33]. R. J. Schoelkopf, P. Wahlgren, A. A. Kozhevnikov, P. Delsing, and D. E. Prober, "The Radio-Frequency Single-Electron Transistor (RF-SET): A Fast and Ultrasensitive Electrometer," Science, vol 280, pp. 1238-1242, May 22, 1998.

[34]. S. Komiyama, O. Astafiev, V. Antonov, H. Hirai and T. Kutsuwa, "A single-photon detector in the far-infrared range," Nature vol. 405, pp. 405-407, 27 Jan. 2000.

[35]. M.E. MacDonald, E.N. Grossman, "Niobium Microbolometers for Far-infrared Detection," IEEE Trans. on Microwave Theory and Tech., v. 43, no. 4, pp. 893-896, April 1995.

[36]. A. Luukanen, A., E.N. Grossman A.J. Miller, P. Helisto, J.S. Pentila, H. Sipola and H. Seppa, "An ultra-low noise superconducting antenna-coupled microbolometer with a room temperature read-out," submitted to IEEE Microwave and Guided Wave Letters, Jan. 2006.

[37]. P. Kruse, R. Dodson, S. Anderson, L. Kantor, M. Knipfer, T. McManus, A. Wood and T. Rezachek, "Infrared imager employing 160x120 pixel uncooled bolometer array," SPIE Conf. on IR Technology and App. XXIV, San Diego, CA, pp. 572-577, July 1998.

[38]. Golay cell and specs. available from QMC Instruments Ltd., School of Physics and Astronomy, Cardiff University, 5, The Parade, Cardiff, CF24 3YB.

[39]. Millitech, South Deerfield, MA, 01373, point contact Schottky diode detectors series DXQ (no longer available).

[40]. S. Weinreb, R. Lai, N.R. Erickson, T. Gaier, J. Wielgus, "W-band InP wideband MMIC LNA with 30 K noise temperature," IEEE MTT-S Int. Microwave Sym. Digest, vol. 1, pp. 101-104 13-19 June 1999.

[41]. H. Wang, R. Lai, Y.C. Chen, Y.L. Kok, T.W. Huang, T. Block, D. Streit, P.H. Liu, P. Siegel and B. Allen. "A 155-GHz monolithic InP-based HEMT amplifier," MTT-S Int. Microwave Sym. Digest, v. 3, pp. 1275-1278, June 1997.

[42]. E.N. Grossman, A. Luukanen and A.J. Miller, "Terahertz active direct detection imagers," Proc. SPIE vol. 5411, pp. 68-77, 2004.

[43]. P.H. Siegel and R.J. Dengler, "Terahertz Heterodyne Imager for Biomedical Applications," SPIE Conf. on THz and GHz Electronics and Photonics III, vol. 5354, pp. 1-9, San Jose, CA, Jan 25-26, 2004.